Journal Applied Mechanics and Technical Physics, Vol. 37, No. 1, 1996

NUMERICAL MODELING OF A SEPARATED TURBULENT FLOW IN THE NEAR WAKE BEHIND A PLATE

V. M. Kovenya and A. S. Lebedev

UDC 533.6

The flow in a near wake behind a body is one of the most important elements of aerodynamic flow, since it greatly influences the overall flow pattern and, as a consequence, the aerodynamic characteristics of an aircraft and its elements. The structure of flow in a near wake is complex and depends on many factors which involve difficulties in experimental and numerical investigation. A survey of the works on this problem can be found, for instance, in [1–3].

In the most complete statement separated flows can be studied within the framework of averaged Navier–Stokes equations supplemented by a turbulence model. However, the results of numerical experiments in gas dynamics show that the problem of selection of a turbulence model currently does not have a satisfactory solution. Application of the same turbulence model for all flow types and configurations of flown bodies does not provide an adequate flow pattern and acceptable agreement of experimental and theoretical data, so the results of application of a certain turbulence model in numerical simulation of particular flows should also be considered to be information about the features of this model for determining the region of its applicability by subsequent comparison with appropriate experimental data.

In the present work a turbulent flow of a viscous heat-conducting gas behind a vertical edge of a finite-thickness plate is studied numerically within the framework of averaged Navier–Stokes equations supplemented by a semi-empirical turbulence model of the $q-\omega$ type. In the works [4, 5] devoted to the solution of a similar problem for an axisymmetrical case under the assumption of flow laminarity it was found, in particular, that with the growth of the Reynolds number Re the length of the recirculation zone behind the body increases monotonically, and the flow in it is accelerated to the point of appearance of a local supersonic zone. The authors of [6, 7], who obtained a similar phenomenon in a numerical experiment, doubt whether it takes place in real flows, since at great Re the flow becomes turbulent. The calculations carried out in the present work make it possible to determine the Re values (within the accepted turbulence model) at which turbulent flow significantly influences gas motion in the near wake, and the character of the influence.

1. Statement of the Problem. We consider the stationary flow of a viscous compressible heat-conducting gas near the vertical trailing edge of a plate. The flow region (Fig. 1) is bounded by the broken line *ABCDEF*. A no-slip condition and heat insulation regime for temperature are assigned at the plate surface *EFA*. Straight line *ED* is the symmetry axis. A developed boundary layer is specified at the entry boundary *AB*. The flow is considered homogeneous and parallel to the flank surface of the plate at outer boundary *BC*.

As a mathematical model describing the flows in the region under consideration we used averaged Navier-Stokes equations, which in dimensionless form in Cartesian coordinates can be written as follows:

$$\frac{\partial U}{\partial t}+\sum_{j=1}^{2}\frac{\partial W_j}{\partial x_j}=0 \quad \text{or} \quad \frac{\partial f}{\partial t}+\sum_{j=1}^{4}C_j f=F. \tag{1.1}$$

Institute of Computing Technologies, Siberian Division, Russian Academy of Sciences, Novosibirsk 630090. Translated from Prikladnaya Mekhanika i Tekhnicheskaya Fizika, Vol. 37, No. 1, pp. 106–113, January–February, 1996. Original article submitted March 20, 1995.

0021-8944/96/3701-0089 $15.00

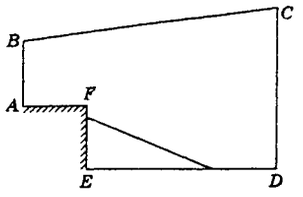

Fig. 1

Here

$$U = \begin{pmatrix} \rho \\ \rho u_1 \\ \rho u_2 \\ \rho E \end{pmatrix}; \qquad W_j = \begin{pmatrix} \rho u_j \\ \rho u_1 u_j + \sigma_{1j} \\ \rho u_2 u_j + \sigma_{2j} \\ \rho E u_j + u_i \sigma_{ij} - q_j \end{pmatrix}; \quad C_j = \left[u_j I - \frac{1}{\rho} \frac{\partial}{\partial x_j} B_j \right] \frac{\partial}{\partial x_j} \qquad (j = 1, 2);$$

$$f = \begin{pmatrix} \rho \\ u_1 \\ u_2 \\ T \end{pmatrix}; \qquad C_{j+2} = \begin{pmatrix} 0 & \delta_{1j}\rho & \delta_{2j}\rho & 0 \\ \delta_{1j}a^2 & 0 & 0 & \delta_{1j}b^2 \\ \delta_{2j}a^2 & 0 & 0 & \delta_{2j}b^2 \\ 0 & \delta_{1j}c^2 & \delta_{2j}c^2 & 0 \end{pmatrix}; \quad a^2 = \frac{1}{\rho}\frac{\partial p}{\partial \rho}; \qquad b^2 = \frac{1}{\rho}\frac{\partial p}{\partial T}; \qquad c^2 = \gamma \frac{p}{\rho};$$

I is an identity matrix; B_j is a diagonal matrix; ρ is the density; u_1 and u_2 are the velocity components; T is the temperature; $E = T + u_j u_j/2$ is the complete specific energy; $p = (\gamma - 1)\rho T$ is the pressure; $\gamma = c_p/c_V = 1.4$.

The stress tensor σ_{ij} and the heat flow q_j are presented in the form

$$\sigma_{ij} = \delta_{ij}\left(p + \frac{2}{3}k\rho\right) - \left(\frac{\mu}{\mathrm{Re}} + \mu_t\right)\left(s_{ij} - \frac{2}{3}\delta_{ij}\frac{\partial u_k}{\partial x_k}\right), \quad q_j = \gamma\left(\frac{\mu}{\mathrm{Pr}\,\mathrm{Re}} + \frac{\mu_t}{\mathrm{Pr_t}}\right)\frac{\partial}{\partial x_j}T,$$

where $s_{ij} = \partial u_i/\partial x_j + \partial u_j/\partial x_i$; μ_t is the turbulent viscosity; k is the turbulent kinetic energy; $\mathrm{Pr} = 0.72$; $\mathrm{Pr}_t = 0.9$.

The turbulent viscosity μ_t is determined by the length scale l and the turbulence rate $q = \sqrt{k}$: $\mu_t = \mu_t(q, l)$. The values of l and q are found from differential equations

$$\frac{\partial}{\partial t}(\rho S_n) + \frac{\partial}{\partial x_j}(\rho S_n u_j) = \frac{\partial}{\partial x_j}\left[\left(\frac{\mu}{\mathrm{Re}} + \frac{\mu_t}{\mathrm{Pr}_n}\right)\frac{\partial S_n}{\partial x_j}\right] + H_n. \tag{1.2}$$

Here $S_n = S_n(l, q)$ $(n = 1, 2)$; $H_n = H_n(\rho, S_1, S_2, \partial u_i/\partial x_j)$ are the source terms; $\mathrm{Pr}_1 = 1$; $\mathrm{Pr}_2 = 1.3$. To close Eqs. (1.1) in the present work we selected a semi-empirical model [8] with two differential equations for $S_1 = q = \sqrt{k}$ and $S_2 = \omega = q/l$. A similar model was used in [9] in numerical simulation of flow near swept-forward and swept-back ledges. The source terms H_n in (1.2) have the form

$$H_1 = \frac{1}{2}\left(c_\mu f J q/\omega - \frac{2}{3}Dq - q\omega\right)\rho, \qquad H_2 = \left[c_1\left(c_\mu J - \frac{2}{3}D\omega\right) - c_2\omega^2\right],$$

where

$$D = \frac{\partial u_k}{\partial x_k}; \qquad J = \left(s_{ij} - \frac{2}{3}\delta_{ij}\right)\frac{\partial u_i}{\partial x_j}; \quad c_1 = 0.405g + 0.045; \qquad c_2 = 0.92; \qquad c_\mu = 0.09;$$

$$g = 1 - \exp\left(-\beta R_T\right); \qquad R_T = \mathrm{Re}\frac{\rho q}{\mu\omega}; \qquad \beta = 0.0018; \qquad \mu_t = c_\mu g \rho q l.$$

2. Numerical Algorithm. The algorithm for numerical solution of Eqs. (1.1) is based on the idea of splitting of the stabilizing operator with respect to physical processes and spatial directions [10]. Replacing the area of continuous variation of an argument by a mesh and determining the values at the mesh nodes we

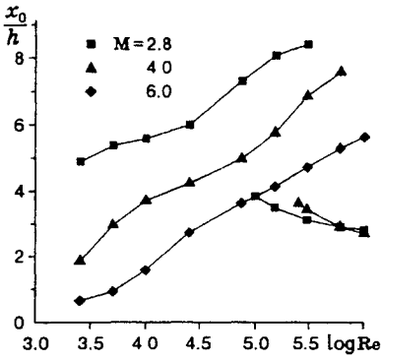

Fig. 2

find a finite-difference analog of Eqs. (1.1):

$$\frac{f^{n+1}-f^n}{\tau}+\sum_{j=1}^{4}C_j^l\left[\alpha f^{n+1}+(1-\alpha)f^n\right]=F_h^n.$$

Here C_j^l is a finite-difference operator that approximates a differential operator C_j with order $O(h^l)$.

After approximate factorization of the stabilizing operator

$$I+\tau\alpha\sum_{j=1}^{4}C_j^l\simeq\prod_{j=1}^{4}(I+\tau\alpha C_j^l)$$

we obtain a system of equations approximating (1.1) in a nondivergent form with order $O(\tau+h^l)$:

$$\prod_{j=1}^{4}(I+\tau\alpha C_j^l)\frac{f^{n+1}-f^n}{\tau}=\sum_{j=1}^{4}C_j^l f^n+F_h^n.$$

A form of finite-difference equations, that is conservative when a stationary solution is achieved is written as

$$\prod_{j=1}^{4}(I+\tau\alpha C_j^l)\frac{f^{n+1}-f^n}{\tau}=-\left(A^{-1}\right)^n\left(W_h^k\right)^n,\quad A=\frac{\partial U}{\partial f},$$

or as a scheme in fractional steps:

$$\xi^n=-\left(A^{-1}\right)^n\left(W_h^k\right)^n,\qquad (I+\tau\alpha C_1^l)\xi^{n+1/4}=\xi^n,$$

$$\cdots\cdots\cdots\cdots\cdots\cdots\cdots\cdots\cdots\cdots$$

$$(I+\tau\alpha C_4^l)\xi^{n+1}=\xi^{n+3/4},\qquad f^{n+1}=f^n+\tau\xi^{n+1}.$$

This scheme approximates system of Eqs. (1.1) with order $O(\tau+\tau h^l+h^k)$ in the nonstationary case and with order $O(h^k)$ in the stationary case. The scheme is conservative in ascertainment and absolutely stable at $\alpha\geqslant 0.5$ for $l=k$. We used earlier a similar finite-difference scheme to solve stationary Navier–Stokes equations by the pseudo-nonstationary method in the simulation of laminar flow in the near wake behind a blunt body of small elongation [4].

Equations (1.2) for determining turbulent parameters were solved independently of (1.1) after each time step using a similar finite-difference scheme. The difference mesh used in the calculations was condensed on the flank surface of the plate and on its base. There were 91 nodes (61 of them fall on the plate base) in the transverse direction with respect to unperturbed flow in the mesh and 97 nodes (21 of them fall on the flank surface of the plate) in the longitudinal direction.

3. Calculation Results. The calculations were carried out at the following Mach-number values for free flow M and Reynolds numbers calculated from the values of the gas-dynamic quantities in homogeneous isentropic flow along the plate:

$$\mathrm{M} = 2.8,\ 4.0,\ \text{and } 6.0, \qquad \mathrm{Re} = 2.5\cdot 10^3\text{–}10^6.$$

The plate half-thickness was taken as the length scale. The profiles of the values at the inlet section AB (Fig. 1) were given in the form

$$p = p_e, \qquad v = 0, \qquad \frac{u}{u_e} = \left(\frac{\Delta y}{\delta}\right)^{1/7}, \qquad T = T_e\left[1 + \sqrt[3]{\mathrm{Pr}}\,\frac{\gamma - 1}{2}\mathrm{M}^2\left(1 - \left(\frac{u}{u_e}\right)^2\right)\right],$$

where subscript e denotes the values in an isentropic flow outside the boundary layer; δ is the thickness of the boundary layer (in our calculations $\delta = 1$); Δy is the distance to the plate normal. Near the plate surface the velocity profile was refined in such a way that the friction coefficient calculated by this profile takes the value obtained from the approximate formula

$$c_f = 0.0128\left(\frac{u_e\theta\rho_w\mathrm{Re}}{\mu_w}\right)^{-0.25}, \qquad \theta = \int_0^\delta \frac{u}{u_e}\left(1 - \frac{u}{u_e}\right) dy$$

(subscript w denotes the values at the plate surface). The turbulent parameters in the inlet section were found from the empirical formulas

$$l = \begin{cases} 0.41\sqrt{0.3}\,y, & y \leqslant 0.09\dfrac{\delta}{0.41}, \\ 0.09\sqrt{0.3}\,\delta, & y > 0.09\dfrac{\delta}{0.41}, \end{cases} \qquad k = \frac{u_\tau^2}{0.3}\cos^2\left(\frac{1}{2}\pi\frac{\Delta y}{\delta}\right)$$

$$\left(u_\tau = \left(\frac{|\tau_w|}{\rho_w}\right)^{0.5}, \quad \tau_w = \frac{\rho_e u_e^2 c_f}{2}\right).$$

The effect of the Reynolds number on the length of the separation zone x_0/h is shown in Fig. 2. We note that at M = 2.8 for Re from the range of approximately from 10^5 to $4\cdot 10^5$ for the length of the separation zone two values are presented in the plot, which correspond to the existence of two different stationary solutions of the problem given coinciding governing parameters. The difference between the calculations was that in the selection of an initial field, the upper branch of the plot was obtained when an already found stationary solution for a small Re was selected as an initial field; the results corresponding to the lower branch of the plot were obtained when a stationary solution for a great Re was selected as an initial field. Thus, there is a "hysteresis" with respect to the Reynolds number. The point is that in the considered range of governing parameters the above procedure of constructing the profiles of the values at the inlet section with the growth of Re gives an increase in the coefficient of turbulent viscosity μ_t, which results in a radical transformation of the flow in the near wake, when Re exceeds the critical value.

For M = 4.0, as one can see from Fig. 2, there is also a duality interval of the solution, and with great Re the length of the separation zone decreases sharply. (A circumstance proved by many calculations should be noted: whenever data are chosen as initial, the resulting stationary flow always corresponds to the curves shown in Fig. 2 and no other solutions appear.) For M = 6.0 no reduction of the separation zone length is observed in the considered range of Re. The decrease in the extent of the recirculation zone at great Re corresponds to theoretical notions on the increased ejecting action of a flow converging from a plate, which causes a pressure decrease in the separation zone and thus increases the flow return to the axis.

Figure 3 shows the average bottom pressure related to the pressure in an unperturbed flow $\overline{p}/p_\infty$. For M = 2.8 it increases from 0.504 to 0.577 in the range $2.5\cdot 10^3 \leqslant \mathrm{Re} \leqslant 3\cdot 10^5$, then decreases to 0.370 and 0.365 at $\mathrm{Re} = 6\cdot 10^5$ and 10^6, respectively. At M = 6.0 the relative bottom pressure increases from 0.180 to 0.398 with Re. In the Re range under review for M = 6.0, the turbulent character of the flow does not influence significantly the flow in the region containing the recirculation zone. A further increase of Re requires a

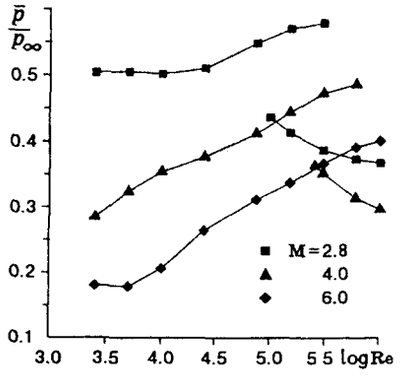

Fig. 3

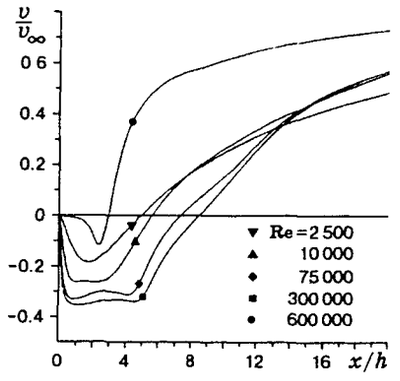

Fig. 4

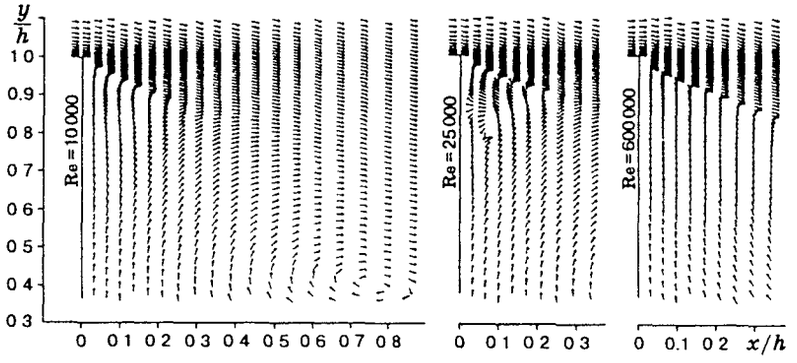

Fig. 5

considerable increase in the number of calculation mesh nodes and, as a consequence, an considerable increase in the computer resources.

Figure 4 shows the velocity distribution v/v_∞ along the symmetry axis at M = 2.8. It is evident that when Re exceeds a certain value not only does the extent of the separation zone decrease abruptly, but the flow pattern in it also changes. Actually, for Re = $6 \cdot 10^5$ the flow in the recirculation zone is distinguished by the fact that the highest velocities occur in the vicinity of the attachment point, and in a certain (rather appreciable) vicinity of the bottom section the motion is very slow (for such regimes the flow region immediately behind the bottom section should be called a "stagnation zone"). The maximum Mach number on the symmetry axis in the separation zone (at M = 2.8) increases from 0.345 to 0.753 with an increase in Re of from $2.5 \cdot 10^3$ to $3 \cdot 10^5$ and decreases to 0.239 at Re = $6 \cdot 10^5$.

Higher velocities in the return flow (to the point of appearance of a local supersonic zone) are obtained in calculating the flow around a blunt axisymmetric body under the assumption of flow laminarity [5]. Supersonic velocities in the recirculation zone have been observed by other authors (for example, in calculating the plane flow behind a cylinder [7]). The calculations made in this work agree with the assumption proposed in [5] that the appearance of local supersonic zones in the return flow behind the body is most likely for flow regimes with a maximum separation-zone length, i.e., when the turbulent flow character has not yet manifested itself as the attachment point of the flow approaches the bottom section.

The direction of the velocity near the corner point for M = 2.8 is shown in Fig. 5. The appearance of a

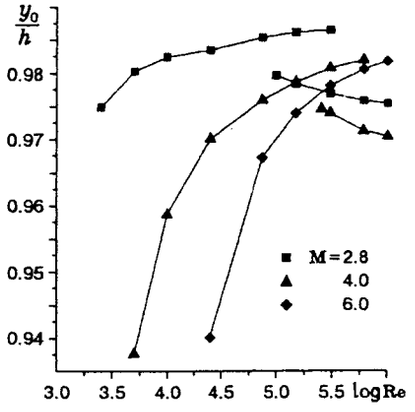

Fig. 6

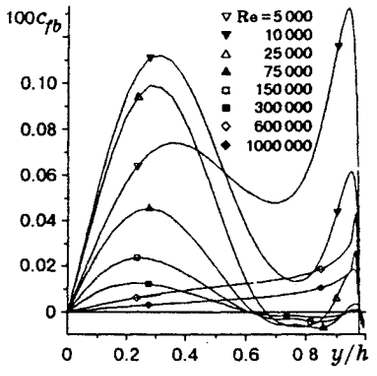

Fig. 7

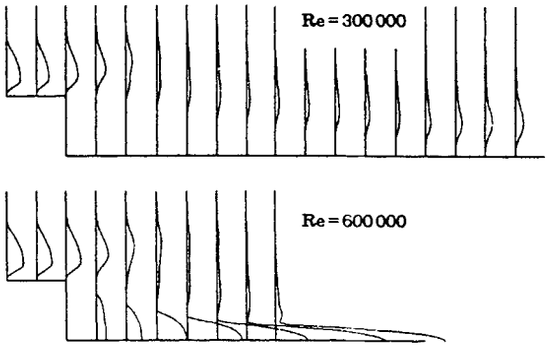

Fig. 8

pair of small-scale vortices rotating in opposite directions in the vicinity of the separation point at the vertical edge of the plate is observed in the present calculations as Re increases, as in the calculations described in [5]. However, these small-scale vortices disappear again when Re reaches $6 \cdot 10^5$. The existence and later disappearance of small-scale vortices with an increase in Re occurs also at M = 4.0. The point of separation of the main flow at the vertical edge with an increase in Re monotonically approaches the conner point, and then slightly recedes from it (Fig. 6).

The position of the separation point was determined by alternating the sign of the friction coefficient $c_{fb} = (2\mu/\mathrm{Re})\ \partial u_\tau/\partial n$, whose distribution along the plate base for M = 2.8 is shown in Fig. 7. A positive value of the coefficient corresponds to motion of a gas away from the symmetry axis. A negative value of the coefficient in the section between the corner point and the separation point is not shown, in view of the zone smallness. Curves in Fig. 7 for $\mathrm{Re} = 6{\cdot}10^5$ and 10^6 are drawn in a scale magnified by 100 with respect to the other curves, which is due to very slow (as mentioned before) gas motion along the plate base for such values of Re.

Profiles of turbulent viscosity μ_t are presented in Fig. 8 in several cross-sections at M = 2.8. For $\mathrm{Re} = 3{\cdot}10^5$ one of two solutions is presented that is relevant to the "laminar" regime with a long separation wave, and for $\mathrm{Re} = 6{\cdot}10^5$ a single solution is presented, which corresponds to the "turbulent" flow regime. As is seen, an essentially different flow pattern in the near wake is caused by the rather insignificant difference between the profiles at the inlet section. Figure 8 shows that after a certain laminarization of the flow when

separating from the plate, it is turbulized again downstream at the wake throat in joining a symmetrical flow. Probably, the degree of flow turbulization at the wake throat at $Re = 6 \cdot 10^5$ exceeds the critical value at which it intensifies the effect on the separation zone, which first results in its slight reduction, increases the flow return to the axis, makes it even more turbulent, etc.

In conclusion we would like to note that the existence of two stationary flow regimes in a certain range of governing parameters corresponding to different regimes of change of the Reynolds number (the increase in Re from small to great values and the decrease in Re from great to small values is a phenomenon of "hysteresis" with respect to the Reynolds number, like "deceleration" of the transition from laminar to turbulent flow) is probably of a physical character and should not depend significantly on the selection of a turbulence model.

This work was supported by the Russian Foundation for Fundamental Research (Grant 93-013-16362).

REFERENCES

1. Paul K. Chang, *Separated Flows* [Russian translation], Mir, Moscow (1972, 1973), Vols. 1–3.
2. L. V. Gogish, V. Ya. Neiland, and G. Yu. Stepanov, "Theory of two-dimensional separated flows," *Itogi Nauki i Tekhniki. Ser. Gidromekh.*, VINITI, Moscow (1975), Vol. 8, pp. 5–73.
3. A. I. Shvets and I. T. Shvets, *Gas Dynamics of a Near Wake* [in Russian], Naukova Dumka, Kiev (1976).
4. V. M. Kovenya and A. S. Lebedev, "Numerical simulation of a viscous separated flow in a near wake," *Prikl. Mekh. Tekh. Fiz.*, No. 5, 53–59 (1989).
5. V. M. Kovenya, A. S. Lebedev, and S. G. Cherny, "Numerical algorithms for solving the Euler and Navier–Stokes equations on the basis of the splitting up method," in: *Computational Fluid Dynamics*, Amsterdam, North-Holland (1988), pp. 718–724.
6. H. Hollanders and D. Devezeaux de Lavergue, "High speed laminar near wake flow calculation by an implicit Navier–Stokes solver," in: *AIAA 8th Computational Fluid Dynamic Conf.* (1987), pp. 598–607.
7. I. V. Egorov and O. L. Zaitsev, "On one approach to numerical solution of the two-dimensional Navier–Stokes equations using through calculation," *Zh. Vych. Mat. Mat. Fiz.*, **31**, No. 2, 286–299 (1991).
8. T. J. Coakley, *A Compressible Navier–Stokes Code for Turbulent Flow Modeling*, New York (1985), (NASA TM 85-899).
9. A. V. Borisov and V. B. Karamyshev, *Method for Numerical Calculation of Separated Turbulent Flows* [in Russian], Preprint No. 9, Inst. Theor. and Appl. Mech., Sib. Div., Russian Acad. of Sciences, Novosibirsk (1988).
10. V. M. Kovenya and N. N. Yanenko, *Splitting Method in Gas Dynamics Problems* [in Russian], Nauka, Novosibirsk (1981).